

Structure of a Tau Class Glutathione *S*-Transferase from Wheat Active in Herbicide Detoxification^{†,‡}

Russell Thom,[‡] Ian Cummins,[#] David P. Dixon,[#] Robert Edwards,[#] David J. Cole,[§] and Adrian J. Laphorn^{*,‡}

Department of Chemistry, University of Glasgow, Glasgow, G12 8QQ, United Kingdom, Department of Biological Sciences, University of Durham, Durham, DH1 3LE, United Kingdom, and Aventis CropScience Ltd., Fyfield Road, Ongar, Essex, CM5 OHW, United Kingdom

Received November 19, 2001; Revised Manuscript Received April 4, 2002

ABSTRACT: Glutathione *S*-transferases (GSTs) from the phi (GSTF) and tau (GSTU) classes are unique to plants and play important roles in stress tolerance and secondary metabolism as well as catalyzing the detoxification of herbicides in crops and weeds. We have cloned and functionally characterized a group of GSTUs from wheat treated with fenchlorazole-ethyl, a herbicide safener. One of these enzymes, *Ta*GSTU4-4, was highly active in conjugating the chemically distinct wheat herbicides fenoxaprop and dimethenamid. The structure of *Ta*GSTU4-4 has been determined at 2.2 Å resolution in complex with *S*-hexylglutathione. This enzyme is the first tau class GST structure to be determined and most closely resembles the omega class GSTs, but without the unique N-terminal extension or active site cysteine. The X-ray structure identifies key amino acid residues in the hydrophobic binding site and provides insights into the substrate specificity of these enzymes.

Glutathione *S*-transferases (GSTs, E.C. 2.5.1.18)¹ are a heterogeneous family of enzymes that catalyze the conjugation of glutathione (GSH) to electrophilic sites on a variety of hydrophobic and usually cytotoxic substrates (1). In plants, GSTs are grouped into four classes based on their amino acid sequences, namely, theta, zeta, phi, and tau (2). While the zeta and theta GSTs are found in plants and animals, the large phi and tau classes of GSTs are unique to plants. The functions of these plant-specific GSTs in the endogenous metabolism of plants remain poorly understood. Recently, particular plant GSTs have been ascribed roles as diverse as oxidative stress tolerance (3), the transport of toxic secondary products (4), and cell signaling during stress responses (5). In contrast, the role of these enzymes in catalyzing the GSH conjugation and hence detoxification of herbicides in both crops and weeds is well characterized (6). In maize (*Zea mays* L.), conjugation with GSH is a major route of metabolism of the selective chloroacetanilide, chloro-*s*-

triazine and thiocarbamate herbicides, with the phi class (termed GSTFs) and tau class (GSTUs) responsible purified and cloned (6). More recently, it has also been recognized that GSTs are important in the metabolism of selective herbicides in bread wheat (*Triticum aestivum* L.). Thus, the chloroacetamide dimethenamid (7), the aryloxyphenoxypropionate fenoxaprop (8), and the sulfonylurea flupyr-sulfuron-methyl (9) are all rapidly detoxified via GSH conjugation in wheat. Such herbicides are used in the field co-formulated with herbicide safeners, compounds that enhance herbicide tolerance in cereal crops by activating the pathways of xenobiotic detoxification, including GSH conjugation (10). Safener-inducible tau class GSTs active in detoxifying dimethenamid and fenoxaprop have been purified from wheat (8), and from *Triticum tauschii* (7), a presumptive diploid donor of the D genome in modern hexaploid wheat (genome AABBDD). Safener-inducible phi class GSTs have also been isolated from wheat (11), although their role in the metabolism of currently used selective herbicides is unclear.

In contrast to the phi class GSTs, no X-ray structures have been reported for the large group of tau class enzymes, which share less than 25% sequence identity with any other GSTs. The molecular characterization of tau class GSTs is of fundamental importance in plants. These enzymes have important roles in determining herbicide selectivity in major crops such as soybean and wheat (6), as well as in intracellular signaling, responses to auxin and cytokinin hormones, and the vacuolar deposition of anthocyanin pigments (reviewed in ref 2). With this in mind, we have determined the first structure of a tau class GST (*Ta*GSTU4-4 from wheat) that has key roles in determining the metabolism and selectivity of the herbicides dimethenamid and fenoxaprop.

* Corresponding author: Department of Chemistry, University of Glasgow, Glasgow G12 8QQ UK. Telephone: 44 0141 330 5940. Fax: 44 0141 330 4888. E-mail: adrian@chem.gla.ac.uk.

[†] The work at both Glasgow and Durham was supported by Aventis Crop Science UK Ltd.

[‡] The crystallographic coordinates have been deposited in the Protein Data Bank with accession code 1GWC.

[‡] University of Glasgow.

[#] University of Durham.

[§] Aventis CropScience Ltd.

¹ Abbreviations: GST, glutathione *S*-transferase; GSTF, phi class GSTs; GSTU, tau class GSTs; GSH, glutathione; DTT, 1,4-dithiothreitol; SDS-PAGE, sodium dodecyl sulfate-polyacrylamide gel electrophoresis; PCR, polymerase chain reaction; TRIS, 2-amino-2-(hydroxymethyl)-1,3-propanediol; aars, amino acid residues; DIG, digoxigenin; EDTA, ethylenediaminetetraacetic acid; GPOX, glutathione peroxidase; EST, expressed sequence tags.

MATERIAL AND METHODS

Purification and Cloning of Tau Class GSTs. Wheat seedlings were treated with or without the safener fenchlorazone-ethyl for 7 days and the tau GSTs present isolated by hydrophobic interaction chromatography (8). The partially purified GSTs were dialyzed against equilibration buffer (20 mM Tris HCl pH 7.8 containing 14 mM 2-mercaptoethanol) and applied at a flow rate of 1 mL min⁻¹ onto affinity columns of *S*-hexylglutathione coupled to epoxy-activated agarose (8). After the sample was washed with equilibration buffer, followed by 20 mM Tris HCl pH 7.8 + 50 mM NaCl, the GSTs were recovered by washing with 20 mM Tris pH 7.8 containing 5 mM *S*-hexylglutathione. The eluted fractions were then applied onto a Q-Sepharose column (Pharmacia Biotech.) and after the sample was washed with 5 column volumes of equilibration buffer, the GSTs were eluted using a linearly increasing concentration of NaCl. Fractions from the Q-Sepharose column containing resolved GST isoenzymes were exhaustively dialyzed with 20 mM Tris/HCl, pH 7.5 containing 0.5 mM DTT and then concentrated using Centricon-10 centrifugal concentrators (Millipore, Watford, UK). The desalted extracts were then assayed for GSH-conjugating activity toward fenoxaprop and the composition of subunits present were analyzed by SDS-PAGE (8). Fractions corresponding to the two major peaks of GST activity toward fenoxaprop were individually formulated with Freund's complete adjuvant and the proteins (100 µg) used to immunize female New Zealand white rabbits. Booster injections, formulated with incomplete adjuvant and each consisting of 100 µg of the respective pure GST, were administered at 40 and 80 days following the initial injection. Serum was prepared 10 days after the final injection and tested for immunoreactivity by immunoblotting of plant extracts resolved by SDS-PAGE (12). A unidirectional cDNA library was prepared in λUNI-ZAP XR (Stratagene) using poly(A)⁺ RNA isolated from safened wheat shoots. After 170 000 plaque forming units were plated out, the cDNA library was immunoscreened using duplicate membrane lifts. One membrane was screened with the anti-TaGSTU1-1 serum and the other with the anti-TaGSTU1-2 serum, essentially as described previously (12). Positively hybridizing plaques were grouped into different classes depending on the intensities of the strength of binding by the antisera and purified through two rounds of screening. The cDNA library was also screened with a digoxigenin (DIG)-labeled DNA probe prepared using PCR and DIG-labeled dUTP using the maize tau GST ZmGSTU3 (12) as a template. The probe was used to screen the cDNA library following standard protocols (Roche UK, East Sussex), involving hybridization carried out at 50 °C using 6× SSC, with the filters then washed at 50 °C with 2× SSC containing 0.1% (w/v) SDS. Following their purification, clones were sequenced in both directions using an ABI automated sequencer; the sequences obtained were analyzed using the BLAST program.

Expression of Recombinant GSTs. The GST clones identified by immunoscreening were expressed in *E. coli* SOLR cells as their respective β-galactosidase fusion proteins using the pBluescript plasmid. When required, these GST coding sequences were also subcloned into the pET11d plasmid for expression of the native recombinant polypeptides. The GST

clone identified using the DNA probe could not be expressed directly as its sequence was out of frame. Restriction sites were introduced using PCR and after subcloning into the PCRScript cloning vector (Stratagene), the native cDNA was ligated into the *Nco*/*Nde* and *Bam* *H*I sites of the pET11 vector. Bacteria transformed with GST cDNAs were cultured for 16 h in LB medium (50 mL) containing 1 mM IPTG and then harvested by centrifugation. Bacteria were re-suspended in 100 mM Tris-HCl, pH 7.5, containing 2 mM EDTA and 1 mM DTT and lysed by ultrasonication. After centrifugation (10000g, 20 min), (NH₄)₂SO₄ was added to 80% saturation and the protein precipitate collected by centrifugation (17000g, 20 min). The recombinant GSTs present were then purified using the combination of *S*-hexylglutathione affinity chromatography and anion exchange chromatography as described for the proteins isolated from wheat shoots.

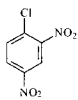
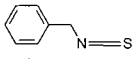
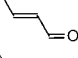
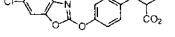
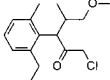
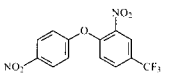
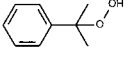
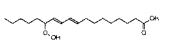
Assay of Recombinant GSTs. After confirming their purity by SDS-PAGE, recombinant GSTs were assayed for GSH-conjugating activity using HPLC based assays for herbicide substrates and spectrophotometric assays for other xenobiotics (12). Glutathione peroxidase (GPOX) activity was determined with cumene hydroperoxide and with linoleic acid hydroperoxide (13-hydroperoxy-*cis*-9, *trans*-11-octadecadienoic acid), the latter being prepared from linoleic acid using soybean lipoxidase (13).

Crystallization, Data Collection, and Processing. Crystals of the native recombinant TaGSTU4-4 were grown by the sitting drop vapor diffusion method. A 1 µL drop of protein solution (10 mg of protein mL⁻¹ in 20 mM Tris HCl, pH 7.5) was mixed with 1 µL of precipitant solution (1.1–1.5 M ammonium sulfate, 0.2 M lithium sulfate, 0.1 M Tris HCl (pH 7.5) containing 5 mM *S*-hexylglutathione) and equilibrated against 0.8 mL of the precipitant solution. Small hexagonal bipyramid crystals were observed after 1 week, growing at best to dimensions of 0.1 × 0.1 × 0.2 mm.

X-ray data were collected from small loop-mounted TaGSTU4-4 crystals (50 × 50 × 100 µm) at the microfocus beamline ID13, ESRF, Grenoble, France, with data extending to 2.2 Å. The crystals were cryocooled using artificial mother liquor containing 20% (v/v) glycerol and flash frozen at 100 K using an Oxford Cryostream Cryosystem. The data were processed using DENZO (14) and scaled using SCALEPACK (15). There were significant problems associated with all attempts to index and scale these data, in particular, the shape of the diffraction spots was variable and a significant fraction of data did not match the predicted spots positions. Attempts were made to process the data using MOSFLM (16) and d*TREK (Molecular Structure Corporation) however these attempts were equally unsatisfactory.

After screening a series of native crystals, a highly redundant data set was collected from a single crystal at Station BM31, EMBL Hamburg, Germany, to 3.0 Å. The streaking of diffraction spots and the mosaicity were lower than previously seen and it was possible to process the data in a hexagonal lattice system unit cell $a = b = 88.0$ Å, $c = 146.8$ Å and $\gamma = 120^\circ$ using DENZO (14). Scaling of the data gave high R_{merge} statistics; however comparison of the statistics for hexagonal, trigonal and C centered orthorhombic spacegroups suggested that the data could be processed in $P6_1/22$ or enantiomorph. The V_m value (17) was calculated to be 3.4 Å³/Da and the solvent content is

Table 1: GST and GPOX Activities of Purified Recombinant Wheat Tau Class GSTs^a

Substrate		Enzyme activity (nkat mg ⁻¹ protein)			
		<i>Ta</i> GSTU1-1	<i>Ta</i> GSTU2-2	<i>Ta</i> GSTU3-3	<i>Ta</i> GSTU4-4
GST activity					
CDNB		1970	8140	30	657
BITC		12.0	1.2	1.5	25.8
Crotonaldehyde		3.7	0.2	0.4	0.1
Fenoxaprop		ND	0.03	0.06	1.06
Metolachlor		0.13	ND	ND	0.43
Fluorodifen		2.00	0.04	ND	0.03
GPOX activity					
Cumene-OOH		1.9	ND	1.1	2.3
Lin-OOH		0.7	0.3	1.5	3.0

^a Results represent the means of duplicate determinations, with variation in the replicates less than 10% in all cases. ND = none detected. The substrates used were 1-chloro-2,4-dinitrobenzene (CDNB), benzylisothiocyanate (BITC), cumene hydroperoxide (cumene-OOH), and linoleic acid hydroperoxide (Lin-OOH). Using CDNB and GSH as substrates, kinetic constants (K_m , k_{cat}) were determined for the *Ta*GSTUs. With respect to GSH for *Ta*GSTU1-1 (0.22 mM, 55.0 s⁻¹), *Ta*GSTU2-2 (0.65 mM, 250.0 s⁻¹), *Ta*GSTU3-3 (0.34 mM, 56.9 s⁻¹), *Ta*GSTU4-4 (0.62 mM, 1.0 s⁻¹) and with respect to CDNB; *Ta*GSTU1-1 (0.87 mM, 191.0 s⁻¹), *Ta*GSTU2-2 (2.13 mM, 667.5 s⁻¹), *Ta*GSTU3-3 (0.21 mM, 14.4 s⁻¹), *Ta*GSTU4-4 (0.58 mM, 1.2 s⁻¹).

estimated to be 63% consistent with a monomer in the asymmetric unit. Table 2. summarizes the data collection statistics.

Molecular Replacement, Model Building, and Refinement. Comparison of the *Ta*GSTU4 sequence with those in the PDB (18) indicated it shared closest identity (21%) with *Zm*GSTF3 (19). Attempts to solve the structure by molecular replacement using the programs AMoRe (20) and EPMR (21) with the low resolution *Ta*GSTU4 data and the coordinates of *Zm*GSTF3, *Zm*GSTF1, or *At*GSTF2 (19, 22, 23) as search models were unsuccessful. When coordinates became available for the human omega GST (24) which share 23% sequence identity with the *Ta*GSTU4 enzyme, the main chain atom coordinates of this model were used as a probe for molecular replacement resulting in a clear solution from the program EPMR. The $2F_o - F_c$ electron density map calculated from this solution was interpretable and enabled a series of features of the *Ta*GSTU4 structure to be built using the program QUANTA (Molecular Simulations Inc.). Two rounds of model building and refinement using the simulated annealing in CNS (25) resulted in an initial model ($R_{cryst} = 33.7$ and $R_{free} = 41.2$) that was used to successfully molecular replace the higher resolution data (2.3 Å) scaled in *P6*₁22. The new data gave significantly improved maps allowing corrections to the Cα backbone and the addition of further side chain atoms. The program ARP (26) was used to add water molecules to the structure and keeping the same R_{free} set as for the 2.9 Å data, the structure was refined using the maximum likelihood refinement program REFMAC (27). Finally, the high-resolution data

were judged to be pseudo *P6*₁22 and were reprocessed as *C22*₁ with unit cell dimensions $a = 88.0$ Å, $b = 152.4$ Å, $c = 146.8$ Å and with three molecules in the asymmetric unit. Final rounds of refinement and building of the essentially complete model were performed in *C22*₁ with medium NCS constraints applied; these resulted in a final R_{cryst} and R_{free} of 15.7 and 21.1%, respectively.

The final model contains three protein monomers each of 221 amino acids, with a molecule of *S*-hexylglutathione and a sulfate in the active site and a total of 711 solvent molecules. The overall quality of the model was assessed using PROCHECK (28) and main chain and side chain parameters were equal to or better than those expected for a 2.3 Å structure. The model shows good stereochemistry with a maximal root-mean-square deviation (rmsd) in the coordinates of 0.2 Å (29) and a final rmsd. from ideal bond lengths and angles of 0.025 Å and 2.3°, respectively (Table 2). The model coordinates have been deposited in the Protein Data Bank with accession code 1GWC (30).

RESULTS

Identification of Safener-Inducible Wheat GSTs Active toward the Herbicide Fenoxaprop. Our previous studies had demonstrated that treatments of wheat seedlings with the herbicide safener fenchlorazole-ethyl markedly enhanced detoxifying GST activities toward several herbicides including the selective aryloxyphenoxypropionate graminicide fenoxaprop (8). These safener-inducible GST activities could be divided into two major groups based on binding affinity to *S*-hexylglutathione. Thus, 62% of the extractable GST

Table 2: Data Collection and Refinement Statistics

data collection	native 1	native 2
source	EMBL X31	ESRF ID13
wavelength (Å)	1.1	0.782
unit cell dimensions (Å)	$a = b = 88.0$ $c = 146.8$	$a = 88.0$ $b = 152.4$ $c = 146.8$
space group	$P6_122$	$C222_1$
resolution (Å)	38.0–3.0	53–2.25
no. of unique reflections	7261	44 559
completeness (%)	99.4	95.4
average multiplicity ^a	12	3
R_{merge} (%) ^b	26.9	11.9
Wilson B (Å ²)	43.2	23.0
Refinement		
resolution range (Å)		30.0–2.25
no. of reflections used		40 929 (all)
R_{cryst} (%) ^c		15.7
R_{free} (%)		21.1
model		
no. of atoms		5115, 93, 711
(protein, hetero, solvent)		
temperature factors (Å ²)		16, 21, 38
(protein, hetero, solvent)		
stereochemistry^d		
Ramachandran quality, % in		
most favored regions		94.9
allowed regions		4.6
rmsd from ideal values		
bond length (Å)		0.025
bond angle (degrees)		2.26

^a Redundancy of data, defined as the ratio of the number of measured and the number of unique reflections. ^b $R_{\text{merge}} = \sum_h \sum_i |I(h,i) - \langle I(h) \rangle| / \sum_h I(h,i)$, where $I(h,i)$ is the intensity value of the i th measurement of h and $\langle I(h) \rangle$ is the corresponding mean value of h for all i measurements of h ; $\sum_h \sum_i$ is the summation over all measurements. ^c $R = \sum_{hkl} (|F_o| - |F_c|) / \sum |F_o|$. ^d Calculated using the program PROCHECK (28).

activity toward fenoxaprop was strongly retained on the affinity matrix, being selectively recovered by elution with S-hexylglutathione. This subgroup of GSTs was composed of at least four distinct isoenzymes, which based on their immuno cross-reactivity to an antiserum raised against maize GSTUs, were all tau GSTs (8).

To identify which isoenzyme(s) had activity toward fenoxaprop, the S-hexylglutathione affinity purified preparations from wheat shoots treated with and without fenchlorazole-ethyl were resolved by anion exchange chromatography. The individual fractions were then assayed for activity toward fenoxaprop (Figure 1). In the preparation from the untreated wheat shoots a single minor peak (I) of fenoxaprop conjugating activity was determined (Figure 1A). In the preparation from the safener-treated shoots, the activity corresponding to peak I was enhanced, representing 31% of the recovered total activity toward fenoxaprop. In addition, a novel second peak (II) of activity was also determined, containing 69% of the fenoxaprop-detoxifying activity. As reported previously (8), when analyzed by SDS–PAGE, peak I in extracts from untreated plants consisted of the TaGST1–1 isoenzyme composed of 25-kDa subunits. In the safener treated samples, peak I contained small amounts of a 24-kDa polypeptide along with elevated concentrations of the 25-kDa TaGST1 subunit (Figure 1c). Analysis of the safener enhanced peak II by SDS–PAGE showed the presence of 25- and 26-kDa subunits present in equal abundance (Figure 1c). The polypeptides present in peaks I and II from safener-treated wheat shoot preparations were then used to immunize rabbits for immunoscreening a cDNA expression library.

Cloning and Functional Characterization of a Group of Tau Class GSTs from Safener-Treated Wheat. The antisera raised against the proteins in peak I and peak II were used to immunoscreen duplicate membranes lifted from a lambda cDNA expression library prepared from wheat shoots treated with 30 μ M of the safener fenchlorazole-ethyl. Following three rounds of screening using the antiserum to peak I, twelve immunoreactive clones were purified and sequenced. In view of their similarity in sequence to other tau class GSTs, notably maize ZmGSTU1, these were collectively termed TaGSTU1 clones. Although the open reading frames were conserved in all 12 clones, three sequence variants were identified in this group in the 5' and 3' untranslated regions and these were individually identified as TaGSTU1a (accession AJ414697), TaGSTU1b (AJ414698), and TaGSTU1c (AJ414699). The sequence of TaGSTU1 encoded a polypeptide of 222-amino acid residues with a predicted molecular mass of 24 974 Da, consistent with the molecular mass of the 25-kDa TaGSTU1 polypeptide observed *in planta* (Figure 1c). Clones corresponding to the safener-inducible 24-kDa GST subunit were not identified by the peak I antiserum, apparently due to failure of the antiserum to recognize this polypeptide. Duplicated screens with the antiserum raised to the peak II proteins identified the same group of 12 plaques obtained using the peak I antiserum. It was concluded that both peak I and peak II contained a common polypeptide antigen, most likely the 25-kDa TaGST1 subunit which appeared to be present in both peaks (Figure 1c). However, the peak II antiserum also identified a further two plaques which on purification and sequencing were found to be significantly different from TaGSTU1, resembling instead the maize tau enzyme ZmGSTU2 (12). These two additional clones were termed TaGSTU2 (accession AJ414700) and TaGSTU3 (AJ414701) respectively and encoded polypeptides of 25 196 Da (233 aars) and 26 412 Da (243 aars) respectively. It was concluded that TaGSTU2 probably corresponded to the 26-kDa polypeptide determined in peak II, while TaGSTU3 could also be present, comigrating during SDS–PAGE analysis with the 25-kDa TaGSTU1 polypeptide (Figure 1D). Since the immunoscreens had identified wheat clones resembling the two maize tau enzymes ZmGSTU1 and ZmGSTU2 it was then of interest to determine if wheat also contained a cDNA resembling ZmGSTU3, the other safener-inducible tau class enzyme identified in maize (12). A DNA probe was prepared to the ZmGSTU3 sequence and used to identify a further distinct tau GST which was termed TaGSTU4. Following sequencing, TaGSTU4 (accession AF004358) was found to encode a polypeptide of 230 amino acids, with a predicted molecular mass of 24 829 Da. On the basis of predicted amino acid sequence, TaGSTU4 was indistinguishable from a safener-inducible tau class GST identified in *T. tauschii* (31). The predicted coding sequences of the tau GSTs cloned from wheat are compared with representative tau class enzymes from *Z. mays*, *Glycine max*, and *Arabidopsis thaliana* in Figure 2.

The TaGSTUs identified by immunoscreening were expressed as the respective N-terminal galactosidase fusion proteins in *Escherichia coli* using the pBluescript vector. TaGSTU4, which had been identified using a DNA probe, was subcloned directly into a pET vector for expression of the native protein. Recombinant GSTs were purified from

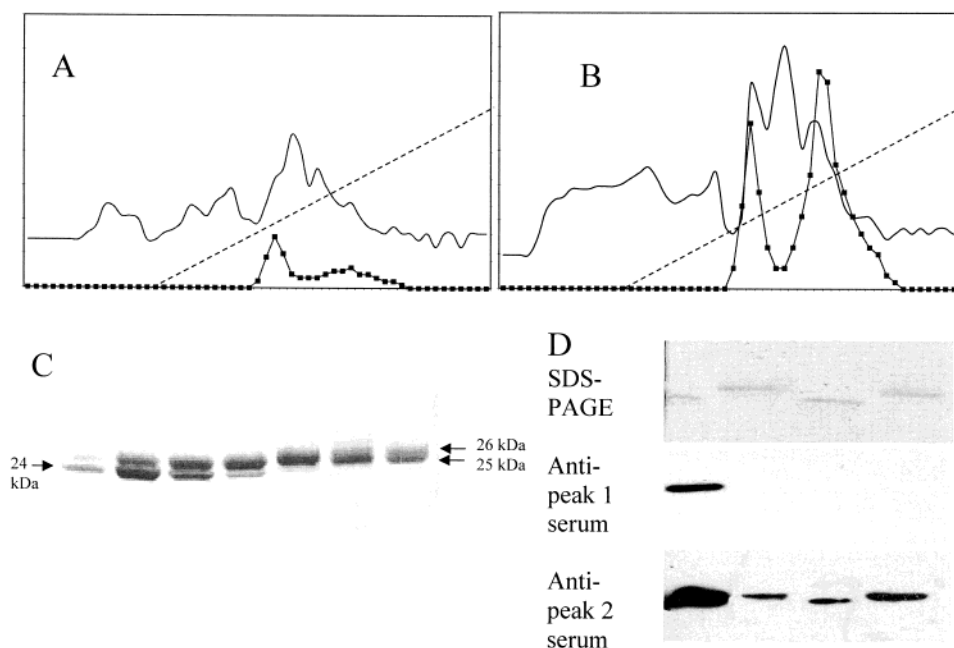


FIGURE 1: Purification of safener-inducible tau class GSTs from wheat active in detoxifying the selective graminicidal herbicide fenoxaprop. The GSTs were purified from identical amounts of protein derived from wheat shoots which were either untreated or treated for 7 days with the safener fenchlorazole ethyl, by a combination of hydrophobic interaction chromatography and *S*-hexylglutathione affinity chromatography. The affinity purified GSTs from (A) the untreated plants and (B) the safener-treated plants were then resolved by Q-Sepharose anion exchange chromatography using an increasing concentration of NaCl (---). The eluate was monitored for UV absorbance at 280 nm (—) and fractions assayed for GST activity toward the herbicide fenoxaprop (■). (C) The GSTs present in peaks I and II were used to raise antisera and their respective polypeptide composition was determined by SDS–PAGE, with the relative mobilities of molecular mass markers indicated. (D) The corresponding recombinant tau class GSTs, *TaGSTU1* (lane 1), *TaGSTU2* (lane 2), and *TaGSTU3* (lane 3) polypeptides were expressed as their respective β -galactosidase fusion proteins using pBluescript while *TaGSTU4* (lane 4) was expressed as the native proteins using the pET vector. The recombinant GSTs were purified as described above and analyzed by SDS–PAGE, prior to immunoblotting with the antisera raised to peak 1 and peak 2, respectively. Note the gal-fusions of the polypeptides analyzed in lanes 1–3 has led to a slight increase in their respective relative molecular masses.

bacterial lysates using *S*-hexylglutathione affinity chromatography followed by anion exchange chromatography, and their purity was confirmed by SDS–PAGE (Figure 1D). When the recombinant GSTs were immunoblotted, *TaGSTU1* was selectively recognized by the antiserum raised to the peak I proteins, while all four GSTUs were recognized by the antiserum raised to peak II (Figure 1d). The purified recombinant GSTs were then assayed for GSH conjugating and glutathione peroxidase (GPOX) activity with a range of substrates (Table 1), which had been previously used in studies with the GSTs purified from wheat seedlings (8). For reference, the general GST substrates CDNB, benzylisothiocyanate, and crotonaldehyde were used, together with the structurally diverse herbicides fenoxaprop, fluorodifen, and metolachlor, representing examples of aryloxyphenoxypropionate, diphenyl ether, and chloroacetanilide chemistries respectively (Table 1). GPOX activity, where organic hydroperoxides are reduced to the respective monohydroxyalcohols using glutathione as reductant (13), was assayed with synthetic cumene hydroperoxide and the naturally occurring linoleic acid hydroperoxide (Table 1). The specific activities of the purified recombinant *TaGSTU1*-1 and the relative activities toward the different substrates were found to be very similar to the values obtained with the *TaGSTU1*-1 isoenzyme purified from wheat shoots (8). Together with the close match in molecular masses for the subunits of the recombinant and plant enzymes, this further confirmed that the *TaGSTU1* clones represented the major constitutive tau GST in wheat. The similarity in specific activities of recombinant and plant homodimers also strongly suggested

that the galactosidase fusions did not significantly affect the catalytic activity of these GSTs.

The recombinant *TaGSTUs* showed overlapping activities toward many substrates, with all GSTs having low, but measurable, activities as GPOXs (Table 1). As determined for the corresponding enzyme from wheat shoots, recombinant *TaGSTU1*-1 showed no detectable activity toward fenoxaprop. However, *TaGSTU1*-1 was highly active toward fluorodifen, a substrate selectivity also observed in the respective enzyme in wheat (8), as well as the related *ZmGSTU1*-1 in maize (12). The recombinant *TaGSTU2*-2 and *TaGSTU3*-3, which had been identified by library immunoscreening using the antisera to the safener inducible GSTs in peak II, showed low activities toward all the herbicides tested. It is unclear whether the respective *TaGSTU2*-2 and *TaGSTU3*-3 homodimers are expressed in planta. Instead, the available evidence suggests that in peak II (Figure 1b), the respective safener-inducible subunits associate with the *TaGSTU1* subunit to form the *TaGSTU1*-2 and *TaGSTU1*-3 heterodimers, respectively (8). Significantly, when the specific activities of the recombinant *TaGSTU1*-1, *TaGSTU2*-2, and *TaGSTU3*-3 were compared to the detoxifying activities present in peak II, it was apparent that the plant isoenzymes purified in this fraction must contain additional GST polypeptides that were more active in detoxifying fenoxaprop and metolachlor. Thus, the peak II GSTs isolated from safener-treated wheat (Figure 1b,c), had specific activities of 0.4 nkat (mg of protein)^{−1} toward fenoxaprop, 0.3 nkat (mg of protein)^{−1} toward metolachlor, and 0.3 nkat mg^{−1} toward fluorodifen. Since the enzyme

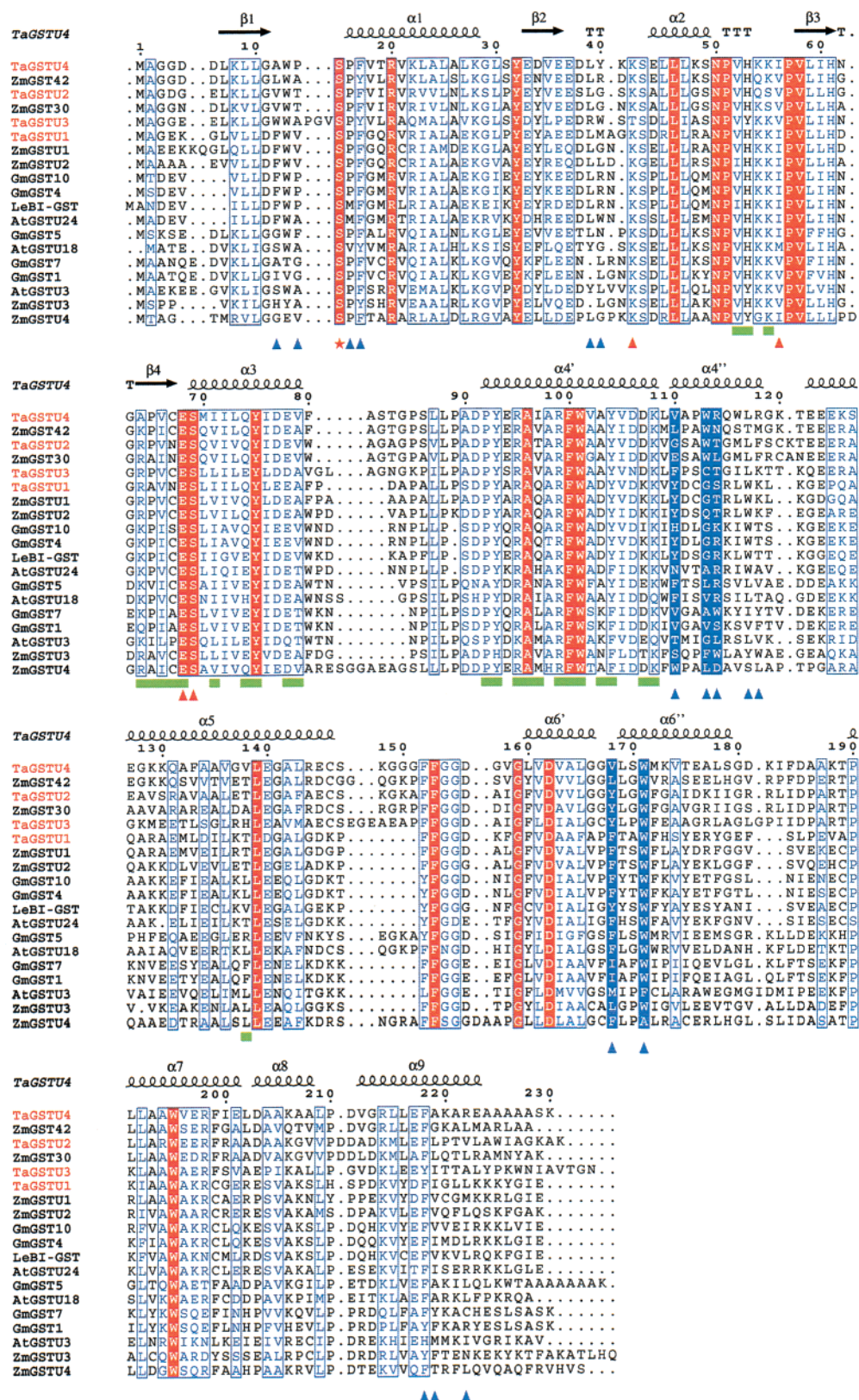


FIGURE 2: A sequence alignment produced using ESPrpt (50) of the four *TaGST*s reported here (highlighted in red) compared with representative tau class GST sequences and with the secondary structure of *TaGSTU4*. Alpha helices and beta strands are represented as helices and arrows, respectively, and beta turns are marked with TT. The proposed catalytic residue, Ser18 is marked * in red, residues involved in binding glutathione are marked with ▲ in red. Residues forming the H-site are marked with ▲ in blue with those considered important to substrate specificity are highlighted in blue. The residues buried at the dimer interface are marked ■ in green. This sequence alignment was created using the following sequences (Organism, Genbank accession numbers or other source in brackets) ZmGSTU1 (*Zea mays*, Y12862); ZmGSTU2 (*Z. mays*, AJ010439); ZmGSTU3 (*Z. mays*, AJ010440); ZmGST30 (*Z. mays*, Q9FQA9); ZmGST42 (*Z. mays*, Q9FQ97); ZmGSTU4 (*Z. mays*, U14599); GmGST1 (*Glycine max*, J03197, M20363); GmGST4 (*G. max*, Q049235); GmGST5 (*G. max*, Q9QF73); GmGST7 (*G. max*, Q9QF1); GmGST10 (*G. max*, Q9QE8); LeBI-GST (*Lycopersicon esculentum*, Q9SE30); AtGSTU24 (*Arabidopsis thaliana*, AAD50016.1); AtGSTU18 (*A. thaliana*, Q9FUS9); AtGSTU3 (*A. thaliana*, Q9ZW28).

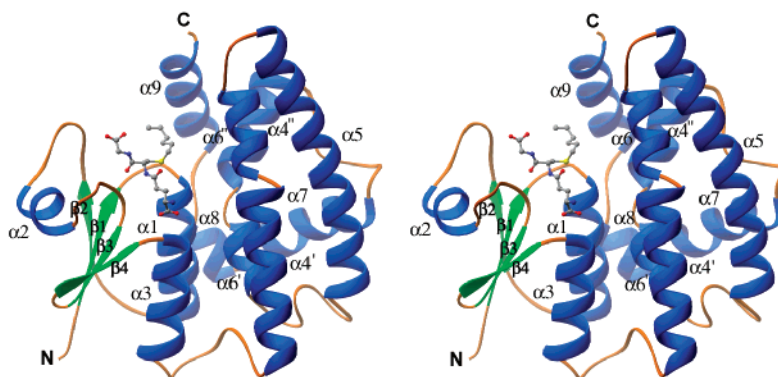


FIGURE 3: A stereo cartoon representation of *TaGSTU4* monomer. α -Helices are drawn as blue ribbons, β -strands are in green arrows. The inhibitor *S*-hexylglutathione is represented as ball-and-stick colored according to atom type. The figure was produced using Ribbons (51).

activities of heterodimeric tau class GSTs are a composite of the activities of the individual subunits (12), the activity toward fluorodifen could be explained by the presence of the *TaGSTU1* polypeptide, which shows high activity toward this herbicide (Table 1). In contrast, *TaGSTU1*, *TaGSTU2*, and *TaGSTU3* containing GSTs have low or nondetectable conjugating activities toward metolachlor and fenoxaprop (Table 1). It was therefore concluded that while peak II contains *TaGSTU1*, and probably both *TaGSTU2* and *TaGSTU3* polypeptides, that these subunits only make a modest contribution to the detoxifying activity toward chloroacetanilide and aryloxyphenoxypropionate herbicides. Instead, peak II must also contain an additional GST, composed of either 25- or 26-kDa polypeptides, highly active in conjugating metolachlor and fenoxaprop. Significantly, the 25-kDa *TaGSTU4* polypeptide was associated with high conjugating toward these two herbicides (Table 1). In addition, the antiserum raised to the polypeptides present in peak II recognized recombinant *TaGSTU4*, suggesting that this polypeptide was present in the original antigen preparation (Figure 1D).

On the basis of its physical properties, immunological activity, and substrate specificity toward herbicides, it seemed likely that an enzyme eluting in peak II containing *TaGSTU4* subunits was a major safener-inducible tau class GST responsible for detoxifying fenoxaprop in wheat. Significantly, the identical GST in safener-treated *T. tauschii* is primarily responsible for the rapid metabolism of the chloroacetamide dimethenamid, a herbicide chemically related to metolachlor (32). Although a detailed kinetic analysis of the recombinant *TaGSTUs* was not undertaken, K_m and k_{cat} values were determined with CDNB and GSH as substrates (Table 1). Although *TaGSTU4-4* was more active than the other *TaGSTUs* in catalyzing the detoxification of fenoxaprop and metolachlor, its turnover rate with CDNB as substrate was considerably lower.

The Structure Determination of *TaGSTU4-4* and Quality of the Final Model. *TaGSTU4-4* was selected for structural elucidation due to its importance in the selective metabolism of the two chemically distinct wheat herbicides, fenoxaprop, and dimethenamid. The purified native recombinant *TaGSTU4-4* was co-crystallized with *S*-hexylglutathione, a model inhibitor of GSTs, via the sitting drop vapor diffusion method and the 2.2 Å resolution structure was solved by molecular replacement using the human omega class GST (24) as a search model. The crystal space group was finally determined to be orthorhombic, $C222_1$, with three polypep-

tides of 221 amino acids in the asymmetric unit. Each chain has a molecule of *S*-hexylglutathione and a sulfate ion bound in the active site, and there are a total of 716 water molecules in the structure. The protein backbone could be clearly traced from Gly4 through to Ala225 in each chain. However, some side chains could not be traced in all of the polypeptides, including Lys120 and Glu123 within the loop region connecting helix $\alpha 4$ to helix $\alpha 5$, Arg118 which could not be traced in monomer B or C, and Glu122 which could not be traced in monomer C. This loop region of the structure exhibited the highest temperature factors within the protein, pointing to its flexibility as observed in the phi class GSTs (22). The final $2F_o - F_c$ electron density map contoured at 1σ is of good quality and shows continuous, well-defined density. The model shows good stereochemistry with an estimated coordinate error (rmsd) of 0.2 Å (29), the parameters for the refined model are summarized in Table 2.

Description of Overall Structure. *TaGSTU4-4* displays the classical GST fold (Figure 3) with the N-terminal domain forming a $\beta\alpha\beta$ element ($\beta 1$ 7–11, $\alpha 1$ 15–29, $\beta 2$ 33–36) connected to a $\beta\beta\alpha$ element ($\beta 3$ 58–61, $\beta 4$ 64–67, $\alpha 3$ 68–80) by an irregular solvent-exposed region which contains a short α -helical section (residues 43–50). The 10-residue linker region (residues 81–90) which joins the N-terminal domain to the larger C-terminal domain folds in a fashion similar to that of the phi class *A. thaliana* GST AtGSTF2 (23) and the human omega class GST (24). In the linker region, a leucine (residue 87) packs between the N- and C-terminal domains rather than an aromatic residue which is observed in other theta class structures. Comparison of the C-terminal domain of *TaGSTU4* with other plant GSTs shows particularly striking differences in the orientation and length of helices $\alpha 4$ (residues 91–119) and $\alpha 5$ (residues 121–147). Helices $\alpha 6$ (residues 159–180), $\alpha 7$, and $\alpha 8$ (residues 189–202 and 202–209) correspond closely to similar regions in most of the other GST classes, while $\alpha 9$ (residues 211–224) folds back over the top of the N-terminal domain in a manner similar to the C-terminus of the human omega class enzyme. Helices $\alpha 4$ and $\alpha 6$ are both interrupted, to keep the naming of the secondary structure consistent with other GST structures the two halves are named α' and α'' (Figures 2 and 3).

The N- and C-terminal domain interface comprises a series of van der Waals interactions between aliphatic residues and two polar interactions Arg20–Asp106 and Gln74–Arg99.

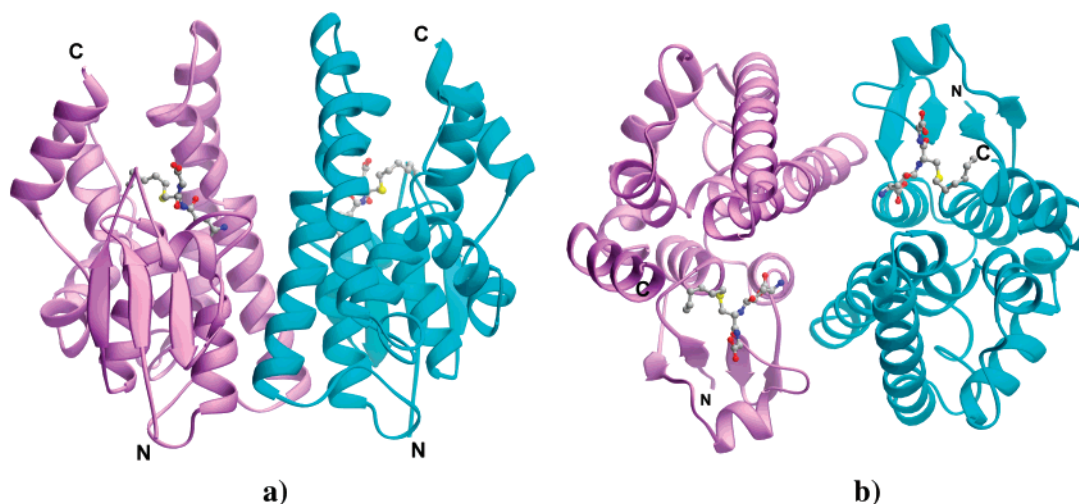


FIGURE 4: A ribbon diagram of the dimeric TaGSTU4 structure, the 2-fold axis relating to the dimer subunits (a) normal to the plane and (b) in the plane of the page, with subunit A colored lilac and subunit B is light blue. The figure was produced using Ribbons (51).

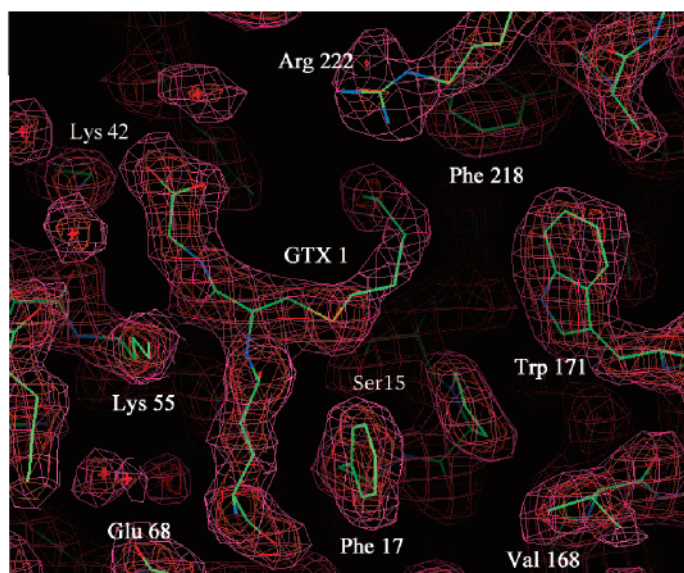
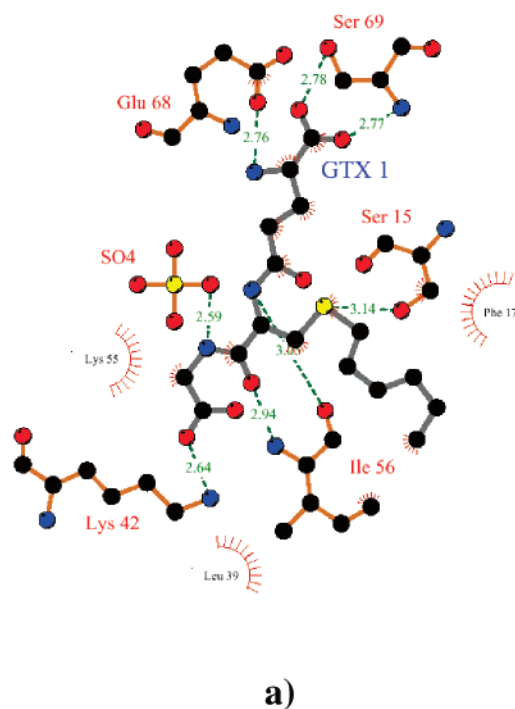


FIGURE 5: (a) A schematic diagram of the interactions between TaGSTU4 and the inhibitor *S*-hexylglutathione generated using LIGPLOT (52). (b) Electron density contoured at 1 and 2 sigma of the active site showing the quality of the data for the *S*-hexylglutathione.

These residues are strongly conserved within the tau class GSTs, but not between tau and phi class GSTs.

Description of the Dimer. The dimer has an atypical open configuration as seen in the human omega enzyme with an interface formed predominately of hydrophobic side chain contacts, exclusively from helices $\alpha 3$, $\alpha 5$, and the beta strand $\beta 4$ from each monomer (Figure 4). The surface accessible area buried at the interface is 2096 Å², comparable with that of the omega class GST (1960 Å²), but significantly smaller than that of most other classes of GST dimer (2700–3400 Å²). Val52 and His 53 from the N-terminal domain of one monomer pack against Phe100, Trp101, and Tyr104 from helix $\alpha 4$ of the second monomer. Additional hydrophobic interactions are formed by Tyr73 of helix $\alpha 3$ that forms an edge-to-face packing arrangement with Tyr93 from helix $\alpha 4$ of the opposite monomer. In addition, the side chain of Tyr93 hydrogen bonds via the hydroxyl to the main chain carbonyl

of Pro65 and a charged interaction is formed close to the crystallographic dyad between the side chain carboxylate of Glu78 and guanidinium groups of Arg95 and Arg99. The residues involved in the dimer interface account for a significant number of the strictly conserved residues in the tau class GSTs (Figure 2).

The GSH Binding Site (G Site). In each monomer, one molecule of *S*-hexylglutathione is bound in the GSH site (Figure 5), the mainly polar nature of the binding of its GSH moiety being consistent with that previously observed in other classes of GST (23, 33–35). The γ -glutamyl moiety is oriented down toward the core of the protein dimer and forms hydrogen bonds with Glu68 (which shows unfavorable Phi/Psi angles in this structure, as is typical for GSTs), the main chain amide of Ser69 and the hydroxyl group of Ser69. In addition, the cysteinyl moiety of the *S*-hexylglutathione molecule forms two hydrogen bonds. One of these is to the

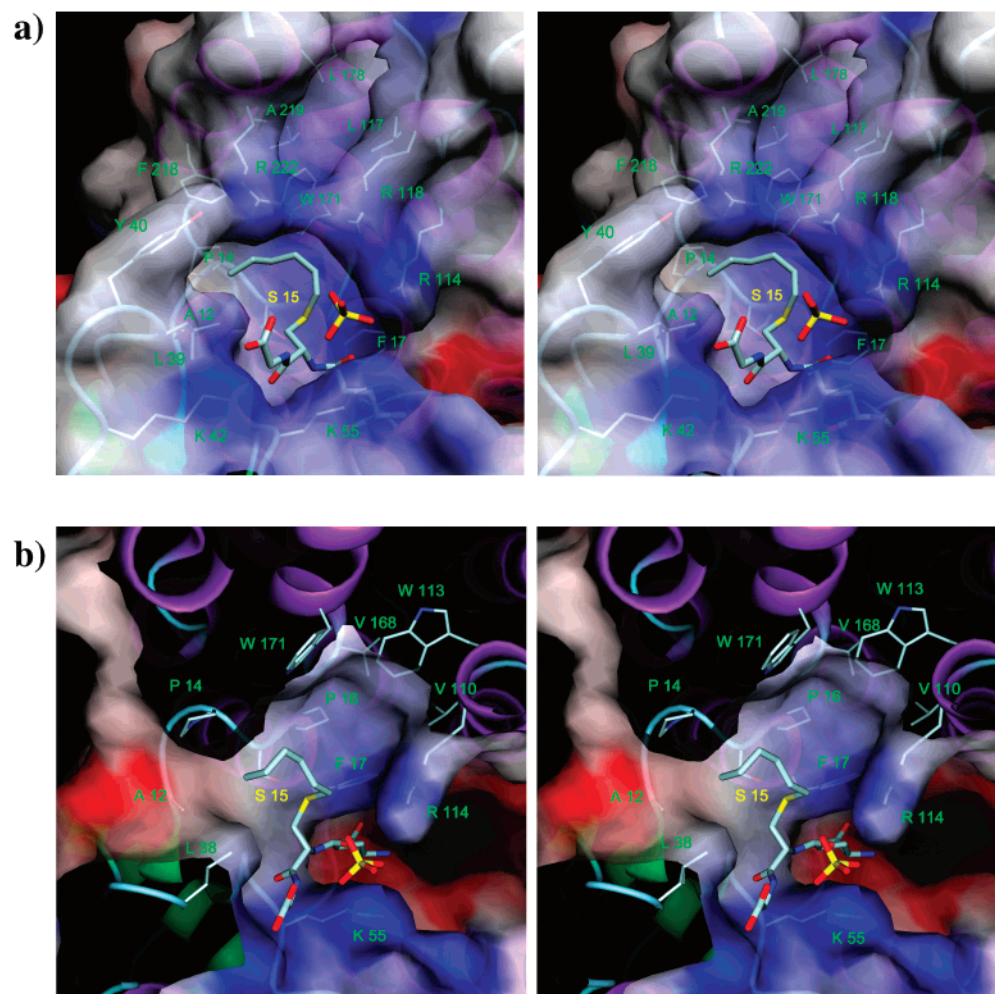


FIGURE 6: Stereoviews of the active site of *TaGSTU4* with the inhibitor *S*-hexylglutathione and a sulfate ion represented as thick sticks, selected active site side chains as thin sticks. The protein is represented as a cartoon with β -strands colored green and α -helices colored purple. Amino acid side chains are labeled in green with the exception of the catalytic serine, which is highlighted in yellow. A transparent surface is colored according to electrostatic potential with saturating colors at 10.0 kT (blue) and -10.0 kT (red) calculated at 298 K and 150 mM salt concentration. Electrostatic calculations and surface were calculated using GRASP (53); the diagram was produced using DINO. (a) An overview of the active site showing it is a large open inverted L shape with a net positive charge around its mouth due to residues Lys42, Lys55, Arg114, Arg118, and Arg222. (b) A more detailed cut away view of the active site highlighting the important amino acid residues implicated in herbicide specificity.

main chain carbonyl of *cis*-Pro57, conserved in all GST structures and crucial for recognition of, and binding to, GSH, while the other is to the amide bond of Ile56 (23, 36–40). A sixth hydrogen bond occurs between the glycyl part of *S*-hexylglutathione and Lys42. As described for the phi class GST structures from *A. thaliana* and *Z. mays* (22, 23), the insect (*Lucilia cuprina*) delta class GST (36) and the human omega class GST (24), there is no interaction between the glutathione portion of the bound ligand and residues of the C-terminal domain. This contrasts with the situation observed in the alpha, beta, mu, pi, sigma, and mammalian theta classes where a salt bridge is typically found between the amino terminal nitrogen of GSH and an acidic residue on helix $\alpha 4$ (24).

The Hydrophobic Binding Site (H Site). GSTs have been shown to bind a wide range of substrates, and this diversity is a reflection of the low degree of sequence identity (and hence structural variation) in the C-terminal domain, which contributes the bulk of the residues involved in binding the electrophiles to be conjugated to GSH. The H-site region within the C-terminal domain is typically hydrophobic in

nature (23, 36–40), with side chain hydrogen bond donors and acceptors fully satisfied. The H-site is large and open and resembles an inverted L in shape, the *S*-hexylglutathione occupying only a small portion of it (Figure 6). Between the N- and C-terminal domains the H-site is open to the solvent via a cavity lined by Ala12, Pro14, Tyr40, and Phe218. Perpendicular to this channel is the main part of the H-site, formed by the residues of $\alpha 6''$ sandwiched on both sides by residues from $\alpha 4''$ and $\alpha 9$. The aromatic amino acids Trp113, Trp171, and Phe218 form the bulk of the molecular surface close to the GSH, with smaller aliphatic residues playing a role further away from the substrate. Interestingly, the topmost region of helix $\alpha 4$ contains two arginine residues (Arg114 and Arg118) which together with Arg222 from helix $\alpha 9$ and Lys42 and Lys55 from the N-terminal domain make the approach to the H-site significantly basic (Figure 6). As a result, a sulfate ion from the crystallization conditions is found in the structure interacting with the amide nitrogen of *S*-hexylglutathione and the side chains of Arg114 and Lys55. Sequence comparison with other tau class GSTs shows that none of the three arginines

(residues 114, 118, and 222) is widely conserved, but the presence of these polar groups capping the H-site may have a significant effect on the substrate specificity of this isoenzyme.

DISCUSSION

Wheat Contains Multiple Tau Class GSTs Involved in Herbicide Detoxification. From their physical properties, immunological relatedness, and enzyme activities of the respective recombinant polypeptides, the four GSTs cloned from wheat encode four major tau class GSTs which are enhanced in wheat shoots following treatment with the herbicide safener fenchlorazole-ethyl (8). These wheat GSTs individually resemble a similar family of safener-inducible tau GSTs in maize (12). Interestingly, in maize phi class GSTs appear to be the dominant class of GSTs, with safener-inducible isoenzymes from this class having major roles in the detoxification of chloroacetanilide and related selective herbicides (6). Although safener-inducible phi class GSTs are present in wheat (11), it appears that the safener-inducible tau class enzymes play the key roles in herbicide detoxification in this crop (7, 8). Similarly, analysis of EST collections has demonstrated that tau class GSTs predominate in soybean with several recombinant enzymes of this class being shown to be active in herbicide metabolism (41). Collectively, these results demonstrate that tau class GSTs have major roles in xenobiotic metabolism in plants. It also demonstrates that GSTs from different classes can substitute for each other's activities in pesticide detoxification in different species, as has been demonstrated for the roles of phi and tau class GSTs involved in anthocyanin deposition in the vacuole (4). In safener-treated wheat, the GSTU-mediated detoxification of the contemporary selective herbicide fenoxaprop was accounted for in two fractions, peak I and peak II, which could be resolved by anion exchange chromatography. The minor proportion of this conjugating activity in peak I appeared to be associated with the appearance of a 24-kDa GST subunit which could not be identified further. However, the dominant conjugating activity toward fenoxaprop residing in peak II was associated with the safener-inducible *TaGSTU4* subunit. Similarly, studies in *T. tauschii* have also shown that the identical enzyme is highly active in detoxifying dimethenamid (9). On the basis of the previous studies with dimethenamid (7, 31, 32), and our studies with fenoxaprop (8), enzymes containing the *TaGSTU4* subunit would make a major contribution to the metabolism of both herbicides in safener-treated wheat. Studies on the origins of *TaGSTU4-4* in modern hexaploid wheat (genome AABBDD) have identified the respective gene as being donated from the diploid progenitor *T. tauschii* (genome DD), where it is localized on the short arm of chromosome 6 (31). Although our studies clearly identified *TaGSTU4-4* as one of the more interesting tau class GST in wheat with respect to its role in determining the detoxification and selectivity of major herbicides, analyses of the enzyme activities of the recombinant GSTs gave few clues as to their functions in endogenous metabolism. Interestingly, unlike safener-inducible phi class GSTs (2), the tau class GSTs identified had low activities as GPOXs, which might have potential functions in counteracting oxidative stress.

Analysis of the Primary Structure of TaGSTU4. To understand the function of tau GSTs in herbicide detoxifi-

cation, as well as to obtain insights into the endogenous functions of this major group of plant GSTs, the 3-dimensional structure of *TaGSTU4-4* was solved by X-ray diffraction. Since the elucidation of the first plant GST structure *AtGSTF2* (23), there have been several publications comparing the phi, zeta, and tau class GSTs using sequence alignments (42, 43). Droog characterized tau class GSTs as having several absolutely conserved sections of sequence, notably, His-Lys-Lys at position 53–55, His-Asn-Gly at position 61–63, Phe153 and Gly159 (with the numbering made consistent with that used with *TaGSTU4*). With the exception of Gly159, these residues are now known not to be conserved either in the many tau GST ESTs reported in crop plants (41) or in the tau wheat sequences presented here. However, they are strongly conserved generally within this GST class and presumably represent important functional residues.

From the *AtGSTF2* structure, Droog proposed that the conserved lysine residues of His-Lys-Lys might interact with the glycyl moiety of glutathione, but this is not observed in the *TaGSTU4* structure. However, in agreement with suggestions based on the *AtGSTF2* structure (44), Glu68, Ser69, and Lys42 are found to interact with glutathione in *TaGSTU4*, even though Lys41 and Lys55 do not. The conserved His-Asn-Gly motif present in the Tau class (43) is shown in the *TaGSTU4* structure to play a role in the orientation of helix $\alpha 3$ with respect to the β -sheet. This is achieved via a number of hydrogen bonds formed between the imidazole of His61 (strand $\beta 4$), the carboxylate of Asp5 (strand $\beta 1$), and the hydroxyl of Tyr75 (helix $\alpha 3$). An additional hydrogen bond to the main chain amide of His6 by Asn62 also stabilizes this loop region. The residue Phe153 is part of the loop region between helices $\alpha 5$ and $\alpha 6$ and is buried in the hydrophobic core, while Gly159 is an invariant residue presumably due to its close proximity to the carbonyl of Leu87 of the linker region.

Structural Comparison. The tertiary structure of *TaGSTU4* was compared with GSTs of the classes: alpha (38), mu (40), pi (45), theta (46), sigma (39), beta (47), phi (23), delta (36), zeta (48), omega (24), and a GST from *Schistosoma japonicum* (49) (Figure 7). The monomer structure of *TaGSTU4* superimposes most closely onto the human omega class GST (24), although it lacks the unique proline-rich segment observed at the N-terminus of the omega class enzyme. The N-terminal domain of *TaGSTU4* shares greatest similarity with the omega, phi, zeta, and theta GST structures; however, the loop structure between strands $\beta 2$ – $\beta 3$ does not contain the aromatic stacking interactions observed in the class phi, theta, and zeta structures (23, 46, 47). The loop instead has leucines (residues 10, 45, and 46) forming the hydrophobic interactions and a network of hydrogen bonds involving the conserved residues Glu37, Ser43, and Ser49. Following this loop region, the conserved *cis*-proline superimposes well on other GST structures to form the characteristic glutathione binding site.

The C-terminal domain of *TaGSTU4* displays some significant differences from the structures of other plant GSTs. Although the helical element $\alpha 4'$ is similar in orientation and length to that previously observed (19, 22, 23), $\alpha 4''$ of *TaGSTU4* is shorter and tilted at an angle of around 25° compared with *AtGSTF2* (23), adopting a conformation more similar to that of the bacterial beta class

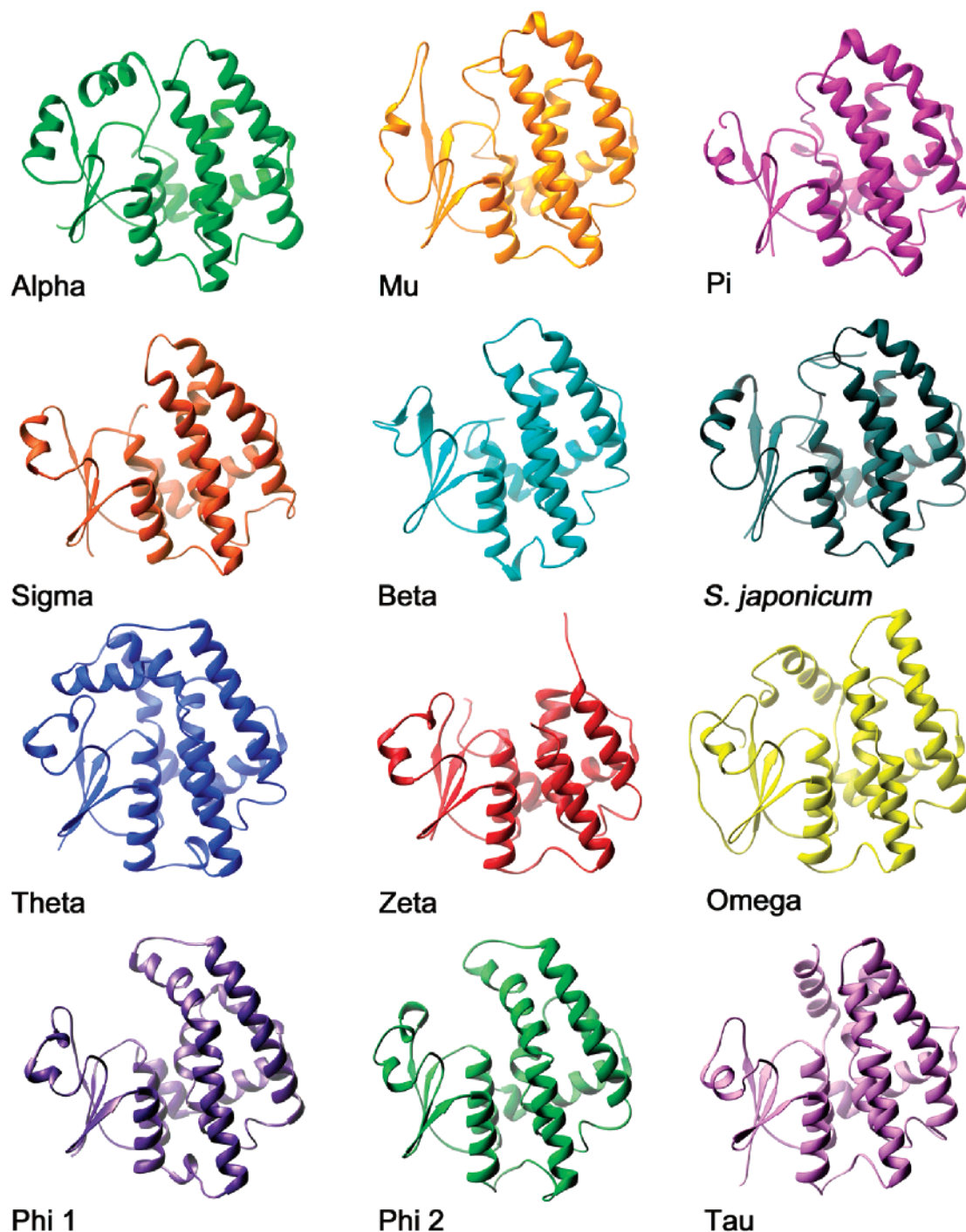


FIGURE 7: A comparison of the various monomer folds of the different classes of the GST superfamily. The structures from different classes were superimposed onto Tau class enzyme *TaGSTU4* using the program LOCK (54) and displayed as differently colored individual ribbons for clarity. The structures superimposed are the plant enzymes phi1 *A. thaliana*, 1gnw (23) (rmsd 1.55 Å over 147 residues); phi2 *Z. mays*, 1axd (22) (rmsd 1.48 Å over 160 residues); zeta, 1e6b (52) (rmsd 1.37 Å over 153 residues); the mammalian enzymes, alpha, 1gse (38) (rmsd 1.69 Å over 140 residues); mu, 4gst (40) (rmsd 1.55 Å over 147 residues); pi, 1gss (49) (rmsd 1.72 Å over 154 residues); theta, 1ljr (50) (rmsd 1.58 Å over 172 residues); omega, 1eem (24) (rmsd 1.34 Å over 179 residues); from other animal classes, sigma, 2gsq (39) (rmsd 1.64 Å over 153 residues); *S. japonicum*, 1gta (53) (rmsd 1.59 Å over 150 residues); and bacterial class beta, 1a0f (51) (rmsd 1.59 Å over 150 residues).

structures (47). This movement of the $\alpha 4''$ – $\alpha 5$ region is due in part to residues Trp116 and Trp113, which are buried against helix $\alpha 6''$. The other secondary structure elements within the C-terminal domain of *TaGSTU4* are generally similar to those of other plant GSTs. The loop between helices $\alpha 5$ and $\alpha 6$ has an unusual sequence in *TaGSTU4* of G–G–G–F–F–G–G with the central two aromatic residues conserved in almost all tau class GSTs. This loop, which

is also present in the omega class enzyme, adopts the same overall conformation as in phi class GSTs but shifted some 3 Å toward helix $\alpha 7$, which is also moved by 1.5 Å. The conserved aspartate (residue 162) found in all GST structures to date, is also present in *TaGSTU4*. The residue is buried in the hydrophobic core of the C-terminal domain, forming hydrogen bonds to the main chain amide groups of Phe153, Gly154, Gly159, and the indole nitrogen of Trp195.

In addition to the different orientation of helices $\alpha 4$ and $\alpha 5$, the most significant feature of the C-terminal domain in *TaGSTU4* is the long C-terminal tail ($\alpha 9$). Although this tail is orientated toward the active site and lies behind it, this does not occlude the active site to the same extent as is observed for the C-terminal helices of the mammalian alpha and theta class GSTs. Although there is little sequence similarity, helix $\alpha 9$ shares significant structural similarity with the human omega class GST both in length and orientation (Figure 7).

Structural Basis for Herbicide Specificity. The first structure of a tau class GST reveals a large inverted L-shaped active site, which is different in shape and size from other plant GSTs described to date. The phi class enzymes structurally characterized have a large rather open cavity between the G- and H-sites, with no C-terminal structure closing off the active site. The H-site has residues exclusively from the long helix $\alpha 4$, which in contrast to *TaGSTU4*, stretches over the front of the H-site, occupying the position of residues from helices $\alpha 6$ and $\alpha 9$ in this structure. There is significant space in the active site of the phi GSTs so that in the case of *AtGSTF2* structure, an additional S-hexylglutathione can bind (23), while maize *ZmGSTF1* binds atrazine in a number of different conformations with contributions from residues in both the N-terminal domain and helix $\alpha 4$ (42). The tau class enzymes have residues from helices $\alpha 6$ and $\alpha 9$ as well as residues from $\alpha 4$ contributing to the H-site. These different residues form the hydrophobic pocket shown in Figure 6b together with residues from the N-terminal domain. The shape of the active site cleft indicates how *TaGSTU4* might bind the herbicide fenoxaprop. The hydrophobic pocket is the correct size to accept the chlorobenzoxazole moiety and position the ester in a position for hydrolysis and conjugation to glutathione. The side chain of Arg118 is well positioned to pi stack against the planar ring system of the benzoxazole. The ester link of fenoxaprop positions the phenyl group of fenoxaprop such that it is likely to interact with Ala12, Pro14, and Leu38 from the N-terminal domain, and the carboxylate moiety most probably forming a salt bridge to Arg222. In herbicides such as dimethenamid, the dimethyl-thiophenyl ring is also likely to be positioned in the hydrophobic pocket (Figure 6b) thereby orienting the reactive chloro group in a position for glutathione addition to occur. The shape of the active site accommodates the branched nature of the structures of these herbicides.

Within the wheat GSTs reported here, there are significant differences in their individual enzyme activities. *TaGSTU4* is the only enzyme to have significant activity toward fenoxaprop; the crystal structure suggests that both Arg118 and Arg222 are important in the binding of this herbicide but are only present in *TaGSTU4*. The GST with the lowest activity toward many of the compounds tested including CDNB, *TaGSTU3*, has an unusual sequence including a unique three-residue insertion before the catalytic serine. These and other sequence differences suggest that this enzyme may not have a primary role in detoxification via glutathione conjugation. *TaGSTU1* is at the sequence level very similar to *ZmGSTU1* and in common with the latter shows activity toward fluorodifen. It can be seen from Figure 2 that the sequence of these enzymes at helix $\alpha 4''$ is significantly different from *TaGSTU4*. At position 110, they have a Tyr instead of a Val, while residues 113 and 114 are

Gly and Ser/Thr, respectively, rather than Trp and Arg. These changes will change significantly the nature of the hydrophobic pocket of the H-site and probably lead to significant movement of the helices $\alpha 4$ and $\alpha 5$.

Comparison of sequence identity of the different plant GSTs alone are not sufficient to predict substrate specificity reliably as has been pointed out by McGonigle and co-workers (41). They highlighted the differences in enzyme activity of three tau class GSTs from soybean, termed *GmGST2*, *GmGST4*, and *GmGST10*, which differ by no more than 11.5% in primary structure. The crystal structure of *TaGSTU4* identifies the important residues which form the active site cleft; comparison of these residues in the three GSTs from soybean show that they have significant changes that can account for their diverse substrate specificities. *GmGST2* has a three-residue deletion in helix $\alpha 6''$ after residue 173 which will affect the folded structure in the active site region, while *GmGST10* has a His at residue 110 in place of Tyr in *GmGST4*, a residue important in forming the hydrophobic pocket of the H-site. It is clear that while determining the substrate specificities of plant GSTs is a significant task, access to the detailed molecular structure of a representative enzyme helps considerably in rationalizing the variety of overlapping specificities shown by these enzymes.

ACKNOWLEDGMENT

Many thanks to members of the Glasgow Protein Crystallography Group for their assistance. We would like to thank Andrew Leslie and Jim Pflugrath for help and time with data processing using the MOSFLM and d*TREK programs, respectively. In addition, we thank the staff of the ESRF, Grenoble, France, and the EMBL, Hamburg, Germany, for help with data collection. We acknowledge the support "European Community - Access to Research Infrastructure Action of the Improving Human Potential Programme" to the EMBL Hamburg Outstation, Contract No. HPRI-1999-00017.

REFERENCES

1. Wilce, M. C. J., and Parker, M. W. (1994) *Biochim. Biophys. Acta*, 1205, 1–18.
2. Edwards, R., Dixon, D. P., and Walbot, V. (2000) *Trends Plant Sci.* 5, 193–198.
3. Kampranis, S. C., Damianova, R., Atallah, M., Toby, G., Kondi, G., Tschlis, P. N., and Makris, A. M. (2000) *J. Biol. Chem.* 275, 29207–29216.
4. Mueller, L. A., Goodman, C. D., Silady, R. A., and Walbot, V. (2000) *Plant Physiol.* 123, 1561–1570.
5. Loyall, L., Uchida, K., Braun, S., Furuya, M., and Frohnmeyer, H. (2000) *Plant Cell* 12, 1939–1950.
6. Edwards, R., and Dixon, D. P. (2000) in *Herbicides and Their Mechanisms of Action* (Cobb, A. H., Kirkwood, R. C., Ed.) pp 38–71, Sheffield Academic Press, Sheffield, UK.
7. Riechers, D. E., Irzyk, G. P., Jones, S. S., and Fuerst, E. P. (1997) *Plant Physiol.* 114, 1461–1470.
8. Cummins, I., Cole, D. J., and Edwards, R. (1997) *Pestic. Biochem. Physiol.* 59, 35–49.
9. Koeppe, M. K., Barefoot, A. C., Cotterman, C. D., Zimmerman, W. T., and Leep, D. C. (1997) *Pestic. Biochem. Physiol.* 59, 105–117.
10. Davies, J., and Caseley, J. C. (1999) *Pestic. Sci.* 55, 1043–1058.
11. Pascal, S., and Scalla, R. (1999) *Physiol. Plant.* 106, 17–27.

12. Dixon, D. P., Cole, D. J., and Edwards, R. (1999) *Plant Mol. Biol.* 40, 997–1008.
13. Graff, G., Anderson, L. A., and Jaques, L. W. (1990) *Anal. Biochem.* 188, 38–47.
14. Otwinowski, Z., and Minor, W. (1997) in *Macromolecular Crystallography, Pt A*, pp 307–326.
15. Otwinowski, Z. (1993) in *Data Collection and Processing* (Sawyer, L., Isaacs, N., and Bailey, S., Ed.) SERC, Daresbury Laboratory, Warrington, UK.
16. Leslie, A. G. W. (1992) in *Joint CCP4 and ESF-EACMD Newsletter on Protein Crystallography*, Daresbury Laboratory, Warrington, UK.
17. Matthews, B. W. (1968) *J. Mol. Biol.* 33, 491–497.
18. Abola, E. E., Sussman, J. L., Prilusky, J., and Manning, N. O. (1997) *Methods Enzymol.* 277, 556–571.
19. Neufeld, T., Huber, R., Reinemer, P., Knäblein, J., Prade, L., Mann, K., and Bieseler, B. (1997) *J. Mol. Biol.* 274, 577–587.
20. Navaza, J. (1994) *Acta Crystallogr. sect. A50*, 157–163.
21. Kissinger, C. R., Gehlhaar, D. K., Fogel, D. B. (1999) *Acta Crystallogr. Sect. D55*, 484–491.
22. Neufeld, T., Huber, R., Dassenbrock, H., Prade, L., and Bieseler, B. (1997) *J. Mol. Biol.* 274, 446–453.
23. Reinemer, P., Prade, L., Hof, P., Neufeld, T., Huber, R., Zettl, R., Palme, K., Schell, J., Koelln, I., Bartunik, H. D., and Bieseler, B. (1996) *J. Mol. Biol.* 255, 289–309.
24. Board, P. G., Coggan, M., Chelvanayagam, G., Eastale, S., Jermini, L. S., Schulte, G. K., Danley, D. E., Hoth, L. R., Griffior, M. C., Kamath, A. V., Rosner, M. H., Chrnyk, B. A., Perregaux, D. E., Gabel, C. A., Geoghegan, K. F., and Pandit, J. (2000) *J. Biol. Chem.* 275, 24798–24806.
25. Brunger, A. T., Adams, P. D., Clore, G. M., DeLano, W. L., Gros, P., Grosse-Kunstleve, R. W., Jiang, J.-S., Kuszewski, J., Nilges, N., Pannu, N.S., Read, R. J., Rice, L. M., Simonson, T., and Warren, G. (1998) *Acta Crystallogr. Sect. D54*, 905–921.
26. Lamzin, V. S., and Wilson, K. S. (1993) *Acta Crystallogr. Sect. D49*, 129–147.
27. Murshudov, G. N., Vagin, A. A., and Dodson, E. J. (1997) *Acta Crystallogr. Sect. D53*, 240–255.
28. Laskowski, R. A., Macarthur, M. W., Moss, D. S., and Thornton, J. M. (1993) *J. Appl. Cryst.* 26, 283–291.
29. Cruickshank, D. W. J. (1999) *Acta Crystallogr. Sect. D55*, 583–601.
30. Berman, H. M., Westbrook, J., Feng, Z., Gilliland, G., Bhat, T. N., Weissig, H., Shindyalov, I. N., and Bourne, P. E. (2000) *Nucleic Acids Res.* 28, 235–242.
31. Riechers, D. E., Irzyk, G. P., Fuerst, E. P., and Jones, S. S. (1997) *Plant Physiol.* 114, 1568.
32. Riechers, D. E., Fuerst, E. P., and Miller, K. D. (1996) *J. Agric. Food Chem.* 44, 1558–1564.
33. Zeng, K., Rose, J. P., Chen, H. C., Strickland, C. L., Tu, C. P., Wang, B. C. (1994) *Proteins* 20, 259–263.
34. Oakley, A. J., Lo Bello, M., Battistoni, A., Ricci, G., Rossjohn, J., Villar, H. O., and Parker, M. W. (1997) *J. Mol. Biol.* 274, 84–100.
35. Garcia-Saez, I., Parraga, A., Phillips, M. F., Mantle, T. J., and Coll, M. (1994) *J. Mol. Biol.* 237, 298–314.
36. Wilce, M. C. J., Board, P. G., Feil, S. C., and Parker, M. W. (1995) *EMBO J.* 14, 2133–2143.
37. Reinemer, P., Dirr, H. W., Ladenstein, R., Huber, R., Lo Bello, M., Federici, G., and Parker, M. W. (1992) *J. Mol. Biol.* 227, 214–226.
38. Sinning, I., Kleywegt, G. J., Cowan, S. W., Reinemer, P., Dirr, H. W., Huber, R., Gilliland, G. L., Armstrong, R. N., Ji, X. H., Board, P. G., Olin, B., Mannervik, B., and Jones, T. A. (1993) *J. Mol. Biol.* 232, 192–212.
39. Ji, X. H., Vonrosenvinge, E. C., Johnson, W. W., Tomarev, S. I., Piatigorsky, J., Armstrong, R. N., and Gilliland, G. L. (1995) *Biochemistry* 34, 5317–5328.
40. Ji, X. H., Zhang, P. H., Armstrong, R. N., and Gilliland, G. L. (1992) *Biochemistry* 31, 10169–10184.
41. McGonigle, B., Keeler, S. J., Lan, S.-M. C., Koeppe, M. K., and O'Keefe, D. P. (2000) *Plant Physiol.* 124, 1105–1120.
42. Neufeld, T., Reinemer, P., and Bieseler, B. (1997) *Biol. Chem.* 378, 199–205.
43. Droog, F. (1997) *J. Plant Growth Regul.* 16, 95–107.
44. Prade, L., Huber, R., and Bieseler, B. (1998) *Structure* 6, 1445–1452.
45. Reinemer, P., Dirr, H. W., Ladenstein, R., Schaffer, J., Gallay, O., and Huber, R. (1991) *EMBO J.* 10, 1997–2005.
46. Rossjohn, J., McKinsty, W. J., Oakley, A. J., Verger, D., Flanagan, J., Chelvanayagam, G., Tan, K. L., Board, P. G., and Parker, M. W. (1998) *Structure* 6, 309–322.
47. Nishida, M., Harada, S., Noguchi, S., Satow, Y., Inoue, H., and Takahashi, K. (1998) *J. Mol. Biol.* 281, 135–147.
48. Thom, R., Dixon, D. P., Edwards, R., Cole, D. J., and Laphorn, A. J. (2001) *J. Mol. Biol.* 308, 949–962.
49. McTigue, M. A., Williams, D. R., and Tainer, J. A. (1995) *J. Mol. Biol.* 246, 21–27.
50. Gouet, P., Courcelle, E., Stuart, D. I. and Metoz, F. (1999) *Bioinformatics* 15, 305–308.
51. Carson, M. (1997) *Methods Enzymol.* 277, 493–505.
52. Wallace, A. C., Laskowski, R. A., and Thornton, J. M. (1995) *Protein Eng.* 8, 127–134.
53. Nicholls, A., Bharadwaj, R., and Honig, B. (1993) *Biophys. J.* 64, A166–A166.
54. Singh, A. P., and Brutlag, D. L. (1997) in *Proceedings of Fifth International Conference on Intelligent Systems for Molecular Biology* (Gaasterland T., K. P., Karpus, K., Ouzounis, C., Sander, C., and Valencia A., Ed.) pp 284–293, The AAAI Press, Menlo Park, USA.

BI015964X